REGULAR ARTICLE

blood advances

ICOS is widely expressed in cutaneous T-cell lymphoma, and its targeting promotes potent killing of malignant cells

Florent Amatore,[1-3] Nicolas Ortonne,[4] Marc Lopez,[1] Florence Orlanducci,[1] Rémy Castellano,[1] Saskia Ingen-Housz-Oro,[5] Amandine De Croos,[4] Clémentine Salvado,[4] Laurent Gorvel,[1] Armelle Goubard,[1] Yves Collette,[1] Réda Bouabdallah,[6] Jean-Marc Schiano,[6] Nathalie Bonnet,[3] Jean-Jacques Grob,[2] Philippe Gaulard,[4] Martine Bagot,[7] Armand Bensussan,[8] Philippe Berbis,[3] and Daniel Olive[1]

[1]Centre de Recherche en Cancérologie de Marseille, INSERM U1068, Centre National de la Recherche Scientifique U7258, Aix Marseille Université, Institut Paoli-Calmettes, Marseille, France; [2]Department of Dermatology and Skin Cancers, Hôpital de la Timone, Aix Marseille Université, Marseille, France; [3]Department of Dermatology, Aix Marseille University, Assistance Publique–Hôpitaux de Marseille, Hôpital Nord, Marseille, France; [4]Department of Pathology and INSERM U955 Team 9 and [5]Department of Dermatology, Assistance Publique–Hôpitaux de Paris (AP-HP), Hôpital Henri-Mondor, Créteil, France; [6]Department of Hematology, Institut Paoli-Calmettes, Marseille, France; [7]Department of Dermatology, Saint-Louis Hospital, AP-HP, Paris University, INSERM U976, Paris, France; and [8]Paris University, INSERM, UMR-976, Institut de Recherche Saint-Louis, Paris, France

Key Points

- ICOS is widely expressed by malignant cells in the skin and blood of patients with CTCL.
- Anti-ICOS ADCs have antitumor potential against CTCL cell lines and patient-derived xenografts.

The treatment of advanced-stage cutaneous T-cell lymphoma (CTCL) remains an unmet medical need. Mogamulizumab, anti-KIR3DL2, and brentuximab vedotin (BV), an anti-CD30 antibody–drug conjugate (ADC) coupled with monomethyl-auristatin-E (MMAE), provided encouraging results, but new targeted therapies are needed. Inducible T-cell costimulator (ICOS), a T-cell costimulatory receptor, is a promising therapeutic target, not only because it is expressed by malignant T cells in CTCL but also because of its connection with the suppressive activity of regulatory T (Treg) cells. Immunohistochemical analysis revealed that ICOS was widely expressed by malignant cells in skin biopsy specimens from 52 patients with mycosis fungoides and Sézary syndrome (SS), as well as in involved node biopsy specimens from patients with SS. Furthermore, flow cytometry demonstrated its strong expression by circulating tumor cells in all our patients with SS. Percentages of $ICOS^+$ Treg cells were significantly higher in patients with SS than in healthy donors. We then investigated the preclinical efficacy of anti-ICOS ADCs generated by coupling murine anti-ICOS monoclonal antibodies with MMAE and pyrrolobenzodiazepine. In 3 CTCL cell lines (Myla, MJ, and HUT78), we observed a significant dose-dependent decrease in cell viability in the presence of anti-ICOS ADCs. In addition, anti-ICOS-MMAE ADCs had an in vitro and in vivo efficacy superior to BV in a mouse xenograft model (MyLa). Finally, we assessed the efficacy of anti-ICOS ADCs in $ICOS^+$ patient-derived xenografts from patients with SS and angioimmunoblastic T-cell lymphoma. Collectively, our findings provide the preliminary basis for a therapeutic trial.

Introduction

Primary cutaneous T-cell lymphomas (CTCLs) account for approximately two-thirds of all primary cutaneous lymphomas,[1] with mycosis fungoides (MF) and Sézary syndrome (SS) being the most common subtypes.[1] Both MF and SS are characterized by a monoclonal proliferation of mature T helper lymphocytes in the skin. Tumor cells in MF are classically $CD3^+CD4^+CD8^-$, with frequent loss of CD7.[2] Sézary cells (circulating malignant lymphocytes) are $CD4^+CD7^-$ and/or $CD4^+CD26^-$ and frequently express CD158k (KIR3DL2).[3] CD158k is the most sensitive marker for detection of Sézary

Submitted 19 May 2020; accepted 20 August 2020; published online 23 October 2020. DOI 10.1182/bloodadvances.2020002395.

For original data, please contact florent.amatore@inserm.fr and daniel.olive@inserm.fr.

The full-text version of this article contains a data supplement.

cells in the blood and skin.[4-6] Programmed death 1 (PD-1) is also expressed by the neoplastic T cells in the skin and blood[7,8] and represents a useful marker for the diagnosis of SS skin lesions.[9] However, the phenotype of Sézary cells varies greatly among patients.[5,10]

The treatment of advanced CTCLs remains an unmet medical need. Brentuximab vedotin (BV),[11] an anti-CD30 antibody–drug conjugate (ADC) linked to monomethyl-auristatin-E (MMAE), does not deliver significant long-term improvements in patient outcomes. More recently, mogamulizumab[12] and anti-KIR3DL2[13] provided encouraging results, but new targeted therapies are needed.

In lymphomagenesis, tumoral T cells can overexpress both costimulatory receptors that allow them to survive, proliferate, and resist apoptosis and coinhibitory receptors that are associated with their functional exhaustion.[14,15] In CTCLs, tumor growth may be driven by both costimulatory and coinhibitory receptors.[16] On the one hand, tumoral and nontumoral CD4 T cells in CTCLs express a wide range of coinhibitory receptors, such as PD-1.[16] On the other hand, in a small cohort of patients with MF, immunohistochemical analysis also revealed the upregulation of costimulatory receptors such as inducible T-cell costimulator (ICOS) on the surface of malignant T cells.[17] More recently, analysis of epidermal and dermal explant cultures of skin biopsy specimens from patients with CTCL revealed that there were more $ICOS^+$ T cells in CTCL samples than in samples from healthy donor skin without, however, specifying the tumoral or reactive nature of these lymphocytes.[16]

ICOS (CD278, AILIM, H4) is a costimulatory receptor for T-cell enhancement and a member of the B7/CD28 receptor superfamily.[18] It is upregulated on activated T lymphocytes (CD4 and CD8 effector, follicular T helper [Tfh], and regulatory T [Treg] cells). Naive T cells express low levels of ICOS but its expression is rapidly induced after T-cell receptor engagement. Its unique ligand, ICOSL, is expressed by antigen-presenting cells, B cells, and many nonhematopoietic cells.[19] The engagement of ICOS by its ligand induces proliferation, survival, differentiation, and cytokine production in order to potentiate the antigen-specific immune response.

The high level of ICOS expression by Tfh-derived tumor cells has been known for ~20 years.[20,21] Malignant cells in angioimmunoblastic T-cell lymphoma (AITL) and primary cutaneous $CD4^+$ small/medium T-cell lymphoproliferative disorder (PCSMTLPD) widely express ICOS. Moreover, activated Treg cells also express ICOS,[19] and $ICOS^+$ Treg cells exhibit a higher immunosuppressive capacity than $ICOS^-$ Treg cells.[22] Recently, Geskin et al[23] identified a high level of Treg cells in the blood of patients with SS. The inhibitory impact of mogamulizumab on Treg cells partly explains its efficacy in SS.[24]

ICOS is therefore a promising therapeutic target due to its wide expression in several peripheral T-cell lymphomas (PTCLs), likely by both malignant T cells and Treg cells. Our first objective was to determine the expression of ICOS in the skin of patients with MF and SS at different stages of the disease and in the blood of patients with SS. Our second objective was to evaluate the efficacy of anti-ICOS ADCs on CTCL cell lines and murine xenograft models.

Materials and methods

Study design and population

We conducted a prospective multicenter study between November 2017 and October 2018.

Patients were >18 years old and signed written informed consent forms prior to the initiation of any procedure related to the study. The diagnosis of CTCL was carried out by a clinician and a pathologist, both members of the French Cutaneous Lymphoma Group (Groupe Français d'Etude des Lymphomes Cutanés). We characterized each patient according to the 2018 WHO-EORTC diagnosis and classification criteria.[25] We then performed clinical staging according to the revised staging system for CTCL based on the tumor-node-metastasis-blood classification system.[26] To confirm a diagnosis of SS, the patient had to meet the criteria of group B2 of the tumor-node-metastasis-blood classification. For functional tests, patients with SS were included either at initial diagnosis or at clinical and biological relapse (B2 criteria). We excluded patients undergoing treatment with immunotherapy or in a therapeutic trial.

Skin samples from 52 patients with CTCL at diagnosis (39 patients) or in relapse (13 patients) were obtained by 4-mm punch biopsy under local anesthesia then fixed with formaldehyde and embedded in paraffin. Blood samples from 13 patients with SS consisted of 15 mL whole blood in EDTA tubes. Skin samples from 12 patients with B-cell lymphoma, 14 patients with $CD30^+$ lymphoproliferative disorder (LPD) (cutaneous anaplastic large cell lymphoma and lymphomatoid papulosis), 12 patients with PCSMTLPD, and 13 patients with AITL were used as control. The clinical characteristics of patients with CTCL and controls are summarized in supplemental Table 1. The healthy volunteers were blood donors at the Etablissement Français du Sang.

All patient tissue collection and research use adhered to protocols approved by the institutional review and privacy boards at Institut Paoli-Calmettes (ICOS-LYMPH-IPC2018003), Saint-Louis Hospital, and the Henri-Mondor Hospital, in accordance with the Declaration of Helsinki.

Generation of monoclonal antibodies (mAbs)

For the generation of anti-ICOS ADCs, a purified murine anti-ICOS antibody generated in our laboratory[27] was sent to Levena Biopharma and Concortis Biotherapeutics (San Diego, CA) for coupling to MMAE and pyrrolobenzodiazepine.

BV (anti-CD30-MMAE) and ado-trastuzumab emtansine (anti-HER2-MMAE) were provided by our hospital pharmacy.

Cell culture

We used 3 CTCL cell lines: MyLa (from N. Ortonne, Department of Pathology, Henri-Mondor Hospital, Créteil, France), MJ (American Type Culture Collection [ATCC]) and HUT78 (ATCC). Myla and MJ are MF cell lines, while HUT78 is a SS cell line. MyLa and HUT78 cells were cultured in RPMI 1640 medium (Life Technologies) supplemented with 10% fetal calf serum, 2% L-glutamine, and 1% pyruvate, and MJ cells were cultured in in Iscove modified Dulbecco medium (Life Technologies) supplemented with 20% fetal calf serum. The diffuse large B-cell lymphoma (Daudi, ATCC CCL-213) and T-cell leukemia (Jurkat, ATCC TIB-152) cell lines were also purchased from ATCC and were cultured in the same way as MyLa

and HUT78 cells. The Jurkat cell line that was transfected to express the ICOS receptor was named Jurkat-ICOS. The MyLa cell line transfected to express luciferase (infection with lentivirus vector expressing LUC2) was named MyLa-luciferase.

Patient-derived xenografts (PDXs) of AITL (DFTL 78024V1) and SS (DFTL 90501V3) were obtained from the Dana-Farber Cancer Institute (Boston, MA).[28]

Flow cytometry and immunochemistry

We used rabbit anti-ICOS antibodies (rabbit polyconal antibody from Spring Biosciences [Abcam, Cambridge, United Kingdom] for immunohistochemistry and SP98 rabbit mAb from Spring Biosciences, with anti-rabbit Alexa488 secondary antibodies), as well as mouse antibodies to PD-1 (NAT105, Abcam), CD4 (4B12, Novocastra) (Leica Biosystems, Wetzlar, Germany), CD8 (C8/144B, Dako) (Agilent Technologies, Santa Clara, CA), and FoxP3 (236A/E7, Abcam) for fluorescent multiplex staining using anti-mouse Texas red secondary antibodies and 4′,6-diamidino-2-phenylindole for nuclear staining. All staining experiments were done on 3-μm-thick sections from formalin-fixed paraffin-embedded skin and node biopsy specimens, either manually or using the Bond Max device (Leica Microsystems). The expression of ICOS and all other markers was scored semiquantitatively and divided into 4 categories based on the proportion of positive cells within the tumoral T-cell infiltrate (0, no staining; low expression, <5%; moderate expression, 5% to 50%; high expression, >50%).

For flow cytometry and functional tests, we used anti-ICOS 314.8 antibodies generated in our laboratory (for details, see Le et al[27]). Other antibodies were purchased from Beckman Coulter (BC; Brea, CA), Becton-Dickinson (BD; Franklin Lakes, NJ), Miltenyi Biotech (Bergisch Gladbach, Germany), and eBioscience (San Diego, CA), including CD45 KO (BC), CD3 percpCy5.5 (BD), CD4 Pacblue (BD), CD7 FITC (BD), CD26 allophycocyanin (APC) (Miltenyi), CD14 APCH7 (BD), CD158e/k phycoerythrin (PE) Vio770 (Miltenyi), CD52 PE (Miltenyi), CD56 APC-Vio770 (Miltenyi), CD19 APC (BD), CD20 PE (BC), CD25 PE-Cf 594 (BD), and FoxP3 FITC (eBioscience).

Flow cytometric analyses were performed on a FACS Canto II (BD Biosciences, San Jose, CA) cytometer. The raw data generated were analyzed with DIVA FACS Canto II software version 8.0.1.

Measurement of cell line viability in the presence of ADCs

Cell viability was measured with alamarBlue (Biosource, Carlsbad, CA). After 4 to 5 days of cell exposure to ADCs, alamarBlue was added. After 4 hours of incubation at 37°C, fluorescence was measured by a luminometer (OPTIMA, BMG Labtech) at a wavelength of 560 nm, as recommended by the manufacturer.

Animals and xenograft models

All experiments were done in agreement with the French guidelines for animal handling, the ARRIVE guidelines, and approved by local ethics committee (agreement no. APAFIS#6069-2016071216263470 v3).

Nonobese diabetic severe combined immunodeficiency γ (NSG/NOD.Cg-Prkdc^{scid} Il2rg$^{tm1Wjl/}$SzJ) male mice of 6 to 8 weeks of age were used for mouse studies and were obtained from Charles Rivers (l'Arbresle, France). Mice were housed under sterile conditions with sterilized food and water provided ad libitum and were maintained on a 12-hour light and 12-hour dark cycle and under temperature and humidity control. Cages contained an enriched environment with bedding material.

Mice were given subcutaneous injections of 8 million Myla or MylaLuc cells in phosphate-buffered saline. Tumor growth was monitored by measuring with a digital caliper and calculating tumor volume (length × width^2 × π/6). When tumors reached an average size close to 100 mm^3, mice were randomized (n = 7 per group) and used to determine the treatment response. Treatments with ADCs were injected IV into the caudal vein. BV and anti-ICOS ADCs were administered at the same dose (3 mg/kg) and adotrastuzumab emtansine at 10 mg/kg. Bioluminescence analysis was performed using a PhotonIMAGER (Biospace Laboratory, Nesles-la-Vallée, France) following addition of endotoxin-free luciferin (30 mg/kg). After completion of the analysis, mice autopsies were performed, and organ luminescence was assessed. Daily monitoring of mice for symptoms of disease (tumor volume >1500 mm^3, significant weight loss, ruffled coat, hunched back, weakness, and reduced mobility) determined the time of killing for injected animals with signs of distress. Survival curves were estimated by the Kaplan-Meier method and compared using the log-rank test.

To explore the efficiency of ADC treatments on lymphoma progression, we used PDXs of AITL (DFTL 78024V1) and SS (DFTL 90501V3). For each PDX, 100 000 to 500 000 cells from the PDXs were injected IV into the caudal vein of NSG mice without prior in vitro culture. When mice were engrafted (human CD45$^+$ cells detected in peripheral blood by flow cytometry), they were treated in the same manner as previously described.

Statistical analysis

All data were analyzed with the GraphPad Prism program (GraphPad Software, San Diego, CA). An unpaired nonparametric Student *t* test with level of significance set at $P < .05$ was used to compare the in vitro efficacy of the antibody of interest and its control. The grouped efficacy analyses were performed with a 2-way analysis of variance test. IC_{50} (median inhibitory dose) was calculated with nonlinear regression. The in vivo survival curves were compared with the log-rank test (Kaplan-Meier).

Results

ICOS is widely expressed by malignant cells in the skin of patients with MF and SS

We used immunohistochemistry to study ICOS expression in skin biopsies of 52 patients with CTCL. In 5 patients with SS, we also analyzed concomitant core biopsies from histologically proven involved nodes with tumor T-cell invasion at histological evaluation (pN3). We measured the ICOS expression of the CD3$^+$ tumoral T-cell population which was characterized morphologically (nuclear atypias) and phenotypically (pan-T-cell antigen loss among CD2, CD5, CD7; PD-1 expression for SS samples; CD30 expression for primary cutaneous CD30$^+$ T-cell LPDs).

Atypical lymphocytic infiltrates in 61% of 23 patients with early-stage MF (stages IA to IIA, without large cell transformation) showed moderate to high ICOS expression. Tumoral cells from 75% of the 12 patients with transformed MF had moderate to high expression of ICOS. Finally, ICOS was highly expressed by 15 out of 17 of the skin biopsies of patients with SS (88%) (Figure 1A-B).

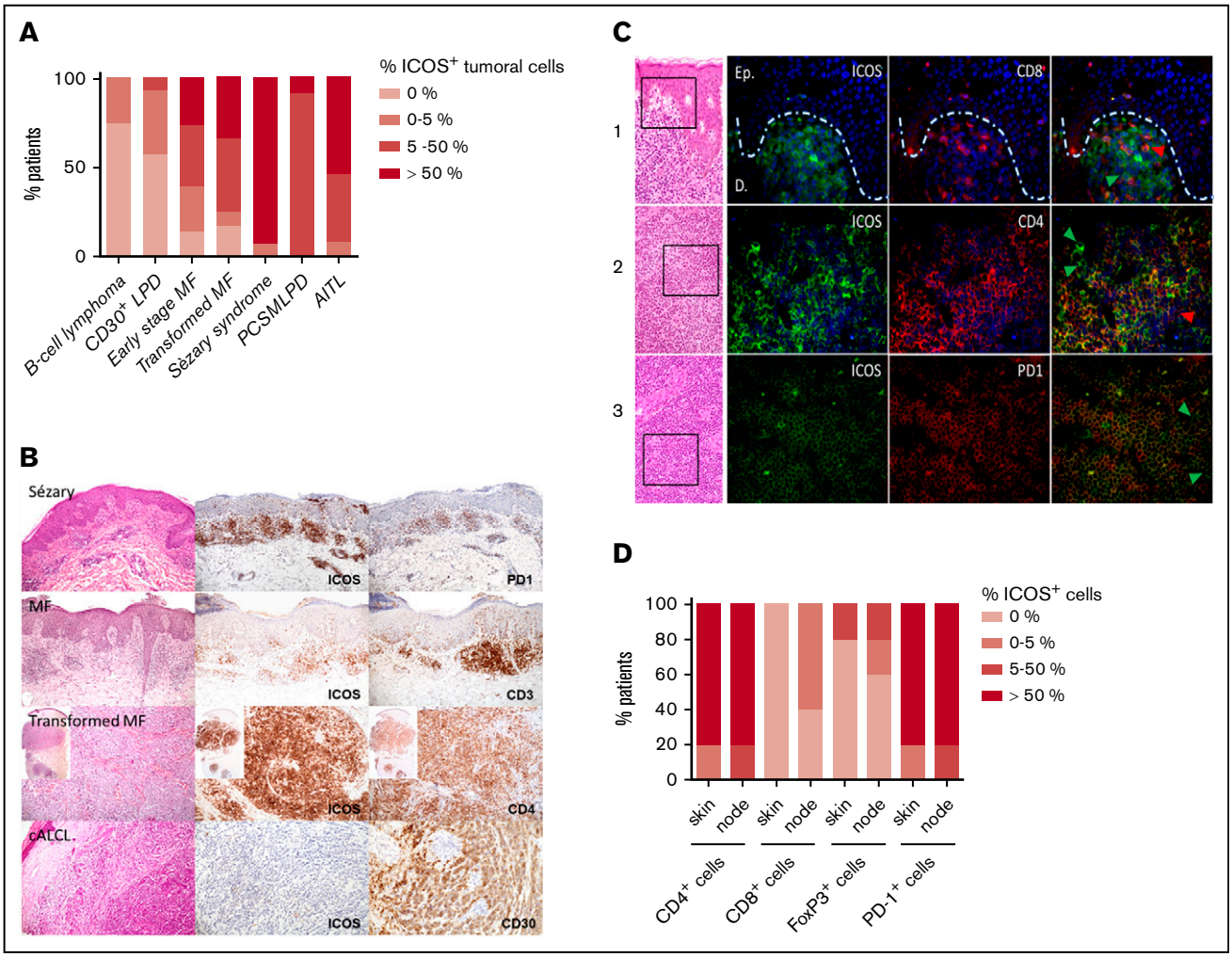

Figure 1. ICOS expression by malignant T cells in CTCL skin biopsy specimens at different disease stages. (A) Percentage of patients with ICOS$^+$ tumoral cells, determined by immunohistochemical analysis of ICOS expression in skin samples of 23 patients with early-stage MF, 12 with transformed MF, 17 with SS, 12 with B-cell lymphoma, 14 with CD30$^+$ LPD (cutaneous anaplastic large cell lymphoma and lymphomatoid papulosis), 12 with PCSMTLPD, and 13 with AITL. Cutaneous B-cell lymphoma skin samples were used as negative controls, whereas PCSMTLPD and AITL were positive controls. (B) Immunohistochemical analysis of the expression of ICOS in epidermal or dermal CD3$^+$CD4$^+$ infiltrating lymphocytes. (C) Double-staining experiments using immunofluorescence with anti-mouse Texas red anti-rabbit Alexa Fluor 488 as secondary antibodies and 4′,6-diamidino-2-phenylindole for nuclear staining in skin (line 1) and lymph node samples (lines 2 and 3) from 3 different patients with SS. Arrowheads identify cells with a single-marker expression; green arrowheads show ICOS$^+$ cells, and red arrowheads show CD8$^+$ cells (line 2) and CD4$^+$ cells (line 3). (D) Double-staining immunohistochemical analysis of skin and node samples of 5 patients with SS. The percentage of patients with ICOS$^+$/CD4$^+$, ICOS$^+$/CD8$^+$, ICOS$^+$/FoxP3$^+$, and ICOS$^+$/PD-1$^+$ cells in the skin and node tumoral infiltrate is represented. cALCL, cutaneous anaplastic large cell lymphoma.

As expected, ICOS was poorly expressed in B-cell lymphoma and widely expressed in PCSMTLPD and AITL tumoral infiltrates. Interestingly, tumoral cells of CD30$^+$ LPD exhibited a low expression of ICOS. Moreover, ICOS was expressed by atypical lymphocytes in all the 5 nodes with SS involvement, being highly expressed in 4 of them. Therefore, ICOS expression increases with the progression of the disease and becomes widely expressed in SS, both in the skin and nodes.

Double-staining experiments were performed in both skin and lymph node samples from these 5 patients to further characterize ICOS expression by neoplastic T cells and the microenvironment (Figure 1C). We observed that most atypical CD4$^+$ T cells (>50%) expressed ICOS, as well as most PD-1$^+$ atypical cells, except for 1 patient with a low to moderate ICOS expression. In the latter, all ICOS$^+$ lymphocytes coexpressed PD-1. A high PD-1 expression was found in all skin and node sample, and ICOS$^+$ PD-1$^-$ lymphocytes appeared to be absent or very rare (<5%). Only very few (<5%) ICOS$^+$CD8$^+$ T cells could be identified in the tumor microenvironment (TME) in 3 node samples. Small to moderate amounts of CD4$^+$ T cells appeared to be ICOS$^-$ in the skin and node samples. A low proportion of FoxP3$^+$ Treg lymphocytes were identified in 3 cases, both in the skin and lymph nodes for 2 and only in the node for one. A low to moderate proportion of them expressed ICOS (Figure 1D). Thus, ICOS expression appears mainly restricted to neoplastic CD4$^+$ T cells, with rare ICOS$^+$CD8$^+$ T cells or FoxP3$^+$ Treg cells in the TME.

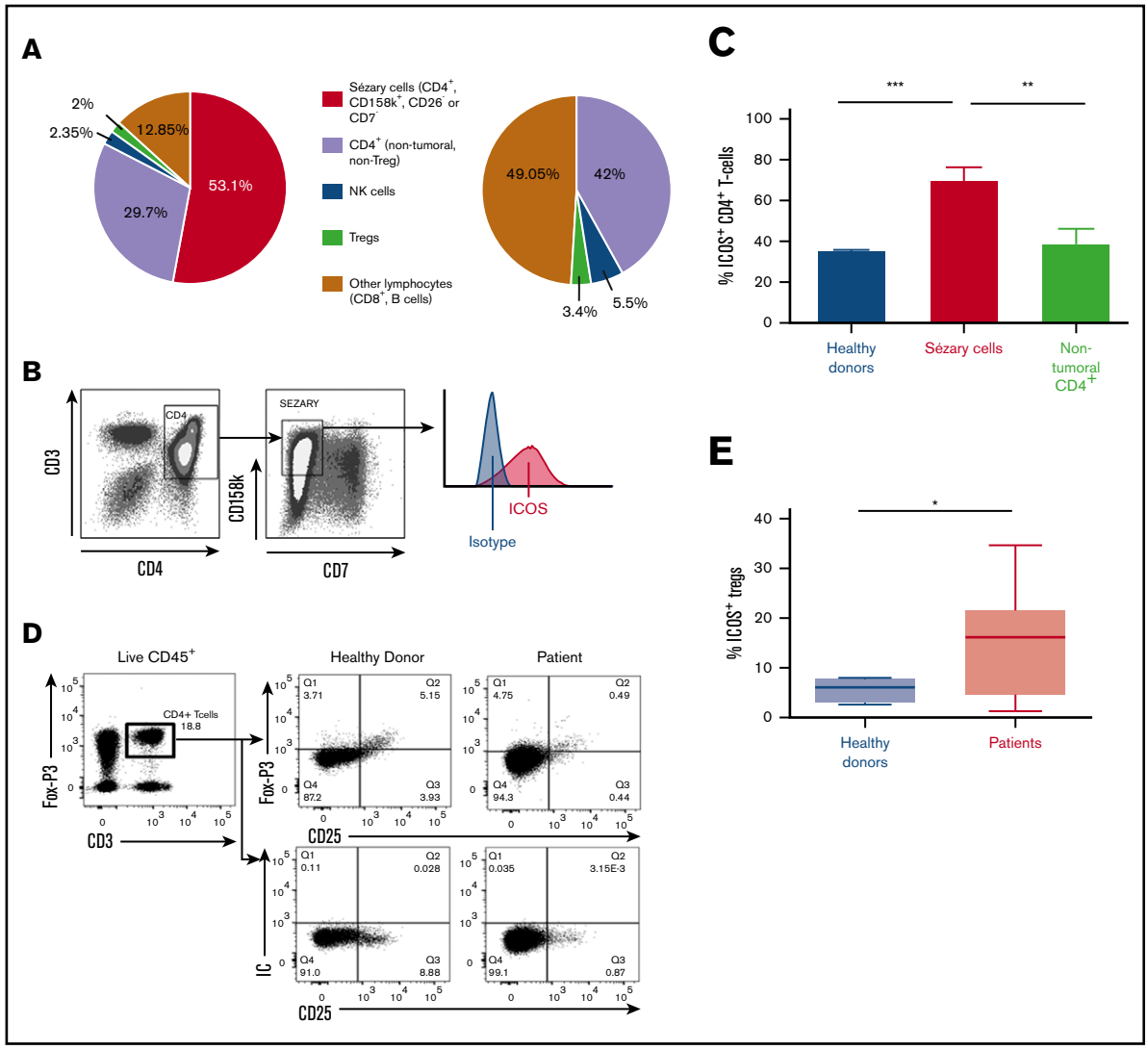

Figure 2. ICOS expression of malignant cells in the blood of patients with SS. (A) Percentages of lymphoid cell populations within peripheral blood of 13 patients with SS and 12 healthy donors using flow cytometry. NK, natural killer. (B) Gating strategy for Sézary cells ($CD4^+CD158k^+CD7^-$) by flow cytometry for a representative patient. (C) Flow cytometric evaluation of ICOS expression in patients with SS and healthy donors. Percentage of $ICOS^+$ cells among Sézary $CD4^+$ T cells and nontumoral $CD4^+$ T cells. Sézary cells were defined as $CD4^+$, $KIR3DL2^+$, $CD7^-$, or $CD4^+$, $KIR3DL2^+$, $CD26^-$. Nontumoral $CD4^+$ T cells are $KIR3DL2^-$. Approximately 70% of Sézary cells expressed ICOS compared with <40% of nontumoral $CD4^+$ cells in patients and $CD4^+$ cells in healthy donors. (D) Gating strategy for Treg cells ($CD4^+FoxP3^+CD25^+$) by flow cytometry for a representative healthy donor and patient. (E) Percentage of $ICOS^+$ Treg cells in patients with SS and healthy donors. ***$P < .001$; **$P = .001$-$.01$; *$P = .01$-$.05$. IC, isotypic control.

ICOS is widely expressed by malignant cells in the blood of patients with SS

ICOS expression by circulating malignant cells was then evaluated using flow cytometry. To ensure the most specific selection of Sézary cells, we considered $CD4^+KIR3DL2^+$ T cells with loss of either CD7 or CD26 to be malignant cells. Figure 2A shows the distribution of lymphocyte populations in 13 patients compared with 12 healthy volunteers. In patients, the median percentage of malignant $CD4^+$ T cells (Sézary cells) among all lymphoid cells was 53.1% (35.9%-71%), meaning that 64% of all $CD4^+$ T cells in patients were malignant cells. Treg cells ($CD4^+CD25^+FoxP3^+$) accounted for 2% of all lymphocytes (ie, 4.3% of nontumoral lymphocytes); this was 3.4% in healthy donors. In addition, natural killer lymphocytes made up 2.4% of all lymphocytes in patients (5% of nontumoral lymphocytes) compared with 5.5% in healthy donors. Natural killer lymphocytes did not express ICOS (data not shown).

Expression of ICOS by circulating tumor cells was found in all patients. The expression was strong; 69% ± 7.3% of tumor cells expressed ICOS vs 38.8% ± 7.1% of nontumoral $CD4^+$ cells in patients ($P < .009$; 95% confidence interval [95% CI], 8.654-51.55) and 31% ± 3.2% of $CD4^+$ cells in healthy volunteers ($P < .0001$; 95% CI, 20.29-46.34) (Figure 2B-C). In patients, 14.4% ± 2.7% of $Foxp3^+CD25^+CD4^+$ Treg cells expressed ICOS compared with 5.6% ± 1.2% in healthy volunteers ($P = .04$) (Figure 2D-E).

Anti-ICOS ADCs mediate killing of MyLa, MJ, and HUT78 cell lines

We first tested anti-ICOS ADCs on MF (MyLa and MJ) and SS (HUT78) cell lines to ensure their functionality. ICOS expression was strong on MyLa (mean fluorescence intensity [MFI] ratio = 143.9) and MJ (MFI ratio = 96) but low on HUT78 (MFI ratio = 4.5). CD30 was highly expressed in all 3 cell lines (Figure 3A; supplemental Figure 1).

We observed a significant dose-dependent decrease in cell viability in the presence of anti-ICOS-MMAE ADCs in the MyLa and MJ cell lines (Figure 3B-C). In the MyLa cell line, anti-ICOS-MMAE ADCs had a better but not statistically significant different IC_{50} values than BV (8.2 ng/mL and 30.6 ng/mL, respectively). In MJ cells, the anti-ICOS-MMAE ADCs tended to be less effective than BV. This difference could be explained by the fact that anti-ICOS mAbs were internalized more in MyLa cells than in MJ cells, while the opposite occurred for anti-CD30 mAbs (supplemental Figure 2).

In HUT78 cells, BV is less effective than in MyLa and MJ (IC_{50} = 251.9 ng/mL), and anti-ICOS-MMAE ADCs exhibit no activity (Figure 3D). Indeed, HUT78 cell line displays resistance to MMAE, as IC_{50} values of free MMAE were 8.2e-007 μM and 0.001 μM in MyLa and HUT78 cells, respectively (supplemental Figure 3). However, anti-ICOS-pyrrolobenzodiazepine ADCs mediate potent killing of the cells, suggesting that anti-ICOS ADCs coupled with a well-adapted drug could be effective even with low levels of ICOS expression.

Finally, we assessed the specificity of ADCs by testing the anti-ICOS ADCs on Jurkat and Jurkat-ICOS cells (Figure 3E-F). IC_{50} values of all the ADCs are summarized in Figure 3G.

In vivo, anti-ICOS-MMAE ADCs are superior to BV in terms of overall survival (OS) and prevents the development of metastases

Mice subcutaneously engrafted with 8.10^6 MyLa cells were randomly assigned to 3 groups: anti-ICOS-MMAE ADC, BV, and anti-HER2 (ado-trastuzumab-emtansine) ADC.

Mice treated with anti-HER2 ADCs died between days 10 and 12. A rapid decline in tumor volume occurred after treatment with anti-ICOS-MMAE ADCs or BV (Figure 4A). Subcutaneous tumor volumes were no longer noticeable from the 15th day after the first injection, with no significant difference between the 2 treatments. Tolerance was excellent, with no evidence of ADC toxicity in treated mice. Interestingly, anti-ICOS-MMAE ADCs provided a longer OS than BV (hazard ratio, 15.2; 95% CI, 3.2-71.1; $P < .0006$) (Figure 4B). The median survival in the BV group was 35 days and was not reached in the anti-ICOS ADC group.

In a second experiment, we aimed to monitor the development of metastases using MyLa-luciferase cells. Twenty-seven mice were engrafted and treated under the same conditions as in the first experiment. On day 25, 7 mice from each group were euthanized and their organs were scanned with the luminometer to detect the presence of metastases. The other mice were maintained until day 40 to detect in vivo the onset of subcutaneous recurrence. On day 25, all mice in the anti-HER2 group had metastases in the lungs, liver, and spleen. In the BV group, ~50% of mice had ≥1 metastasis in 1 of these 3 organs. In the anti-ICOS-MMAE group, the organs did not exhibit significant bioluminescence (Figure 4C-E). On day 40, subcutaneous recurrence was perceived in vivo in mice of the BV group, while mice in the anti-ICOS group were still in remission (Figure 4F).

Anti-ICOS-MMAE ADCs have a potent in vivo efficacy in PDXs of $ICOS^+$ lymphomas

To improve the predictive value of our preclinical model, we assessed the efficacy of anti-ICOS-MMAE ADCs in $ICOS^+$ PDXs from patients with SS and AITL.

$ICOS^+$ PDXs from patients with SS were IV injected into 14 NSG mice. On day 40 after engraftment, we observed a brutal and rapid increase in the number of Sézary cells. We took blood samples from each mouse and quantified the number of circulating tumor cells to evenly distribute the living mice into 2 groups of 7 mice: the anti-ICOS-MMAE ADC group and the anti-HER2 ADC control group. Fifteen days after treatment, the mice were euthanized, and we quantified the number of malignant cells in the blood and organs by flow cytometry. We observed a reduced number of tumor cells in the blood, bone marrow, and spleen of the anti-ICOS ADC group (Figure 5A-C). Anti-ICOS ADCs here show a rapid and significant efficacy, suggesting that this therapeutic strategy could be used in patients with advanced SS.

In a second experiment, $ICOS^+$ PDXs from patients with AITL were IV injected into NSG mice. We subsequently took blood samples to detect tumor cells by flow cytometry. The first tumor cells were detected on day 21 after transplantation, so treatments began on day 22. Mice were treated with anti-ICOS-MMAE ADCs, vincristine (positive control, with the same mode of action as MMAE), or saline solution (NaCl à.9%). Median survival in the negative control and vincristine groups was 67 and 68 days, respectively. Median survival in the anti-ICOS group was not reached. The better survival of mice treated with anti-ICOS ADC compared with those receiving saline solution was highly significant ($P < .0001$) (Figure 5D). No evidence of ADC toxicity was observed in treated mice. On day 120, the mice treated with anti-ICOS ADCs were in complete remission, since no blasts were detectable (data not shown).

Discussion

This study presents the preclinical efficacy results of anti-ICOS ADCs and demonstrates their excellent antitumor potential under several complementary experimental conditions in the context of both CTCL and AITL.

We report for the first time the strong and constant expression of ICOS by circulating Sézary cells, the most severe form of CTCL. In MF skin biopsy specimens, the expression of ICOS appears to increase with disease severity. It should be noted that in early forms of MF, tumor infiltration is mainly composed of the TME's lymphocytes and that this balance is reversed in late forms of the disease.[29]

Further studies are needed to assess the predictive potential of ICOS expression on the evolution and prognosis of CTCL. In many solid cancers, such as melanoma,[30] breast cancer,[31] gastric cancer,[32] and clear cell renal cell carcinoma,[33] the expression of ICOS by TME Treg cells is associated with poor

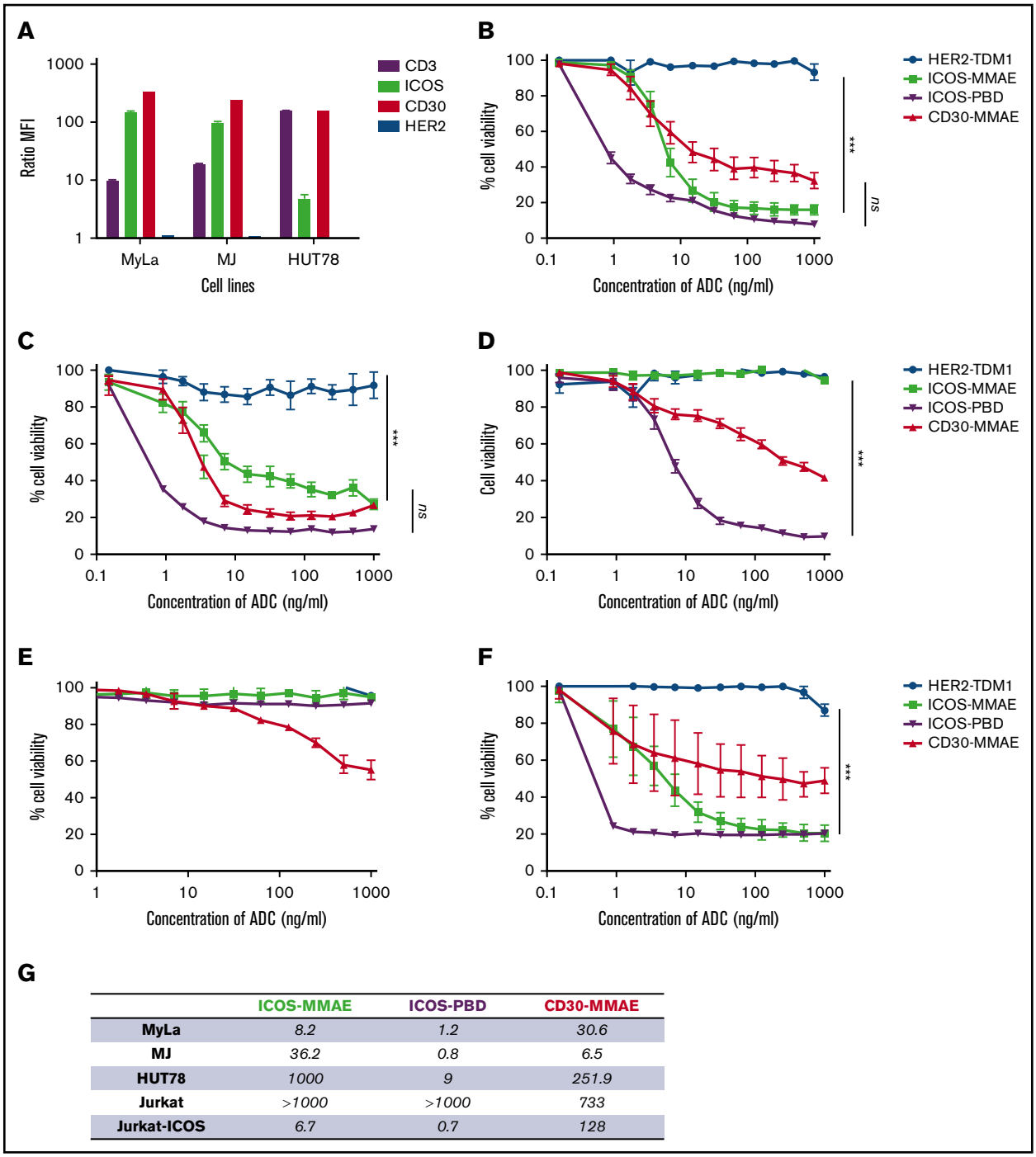

	ICOS-MMAE	ICOS-PBD	CD30-MMAE
MyLa	*8.2*	*1.2*	*30.6*
MJ	*36.2*	*0.8*	*6.5*
HUT78	*1000*	*9*	*251.9*
Jurkat	*>1000*	*>1000*	*733*
Jurkat-ICOS	*6.7*	*0.7*	*128*

Figure 3. Anti-ICOS ADCs have a specific in vitro efficacy in ICOS-expressing cell lines. (A) Immunophenotyping of CTCL cell lines using flow cytometry. Note that ICOS expression was higher in MyLa and MJ cells than in HUT78 cells. (B-F) Percentage of cell viability in increasing ADC concentrations, assessed with alamarBlue (mean of 16 replicates), on MyLa cells (B), MJ cells (C), HUT78 cells (D), Jurkat cells (E), and Jurkat-ICOS cells (F). Anti-HER2 ADCs were used as a negative control, whereas anti-CD30 ADCs (BV) were a positive control. (G) Summary table of IC_{50} values expressed in ng/mL of all ADCs. ***$P < .001$. ns, not significant. PBD, pyrrolobenzodiazepine.

prognosis. The prognostic impact of ICOS has not been evaluated in malignant hematological diseases.

We have shown that anti-ICOS ADCs are effective in ICOS-expressing lymphoma cell lines and PDXs. It is to be expected that they will induce depletion of not only malignant $CD4^+$ T cells and Treg cells but also nonmalignant $CD4^+$ and $CD8^+$ T cells expressing ICOS. Here, we show that nonmalignant $CD4^+$ T cells of patients with SS represent only ~30% of all lymphocytes, of which 30% to 40% express ICOS. Moreover, $CD8^+$ T cells represent <10% of lymphocytes (the CD4/CD8 ratio is classically >10:1 in SS). In CTCL, $CD8^+$ T cells infiltrating the TME are known to be poorly

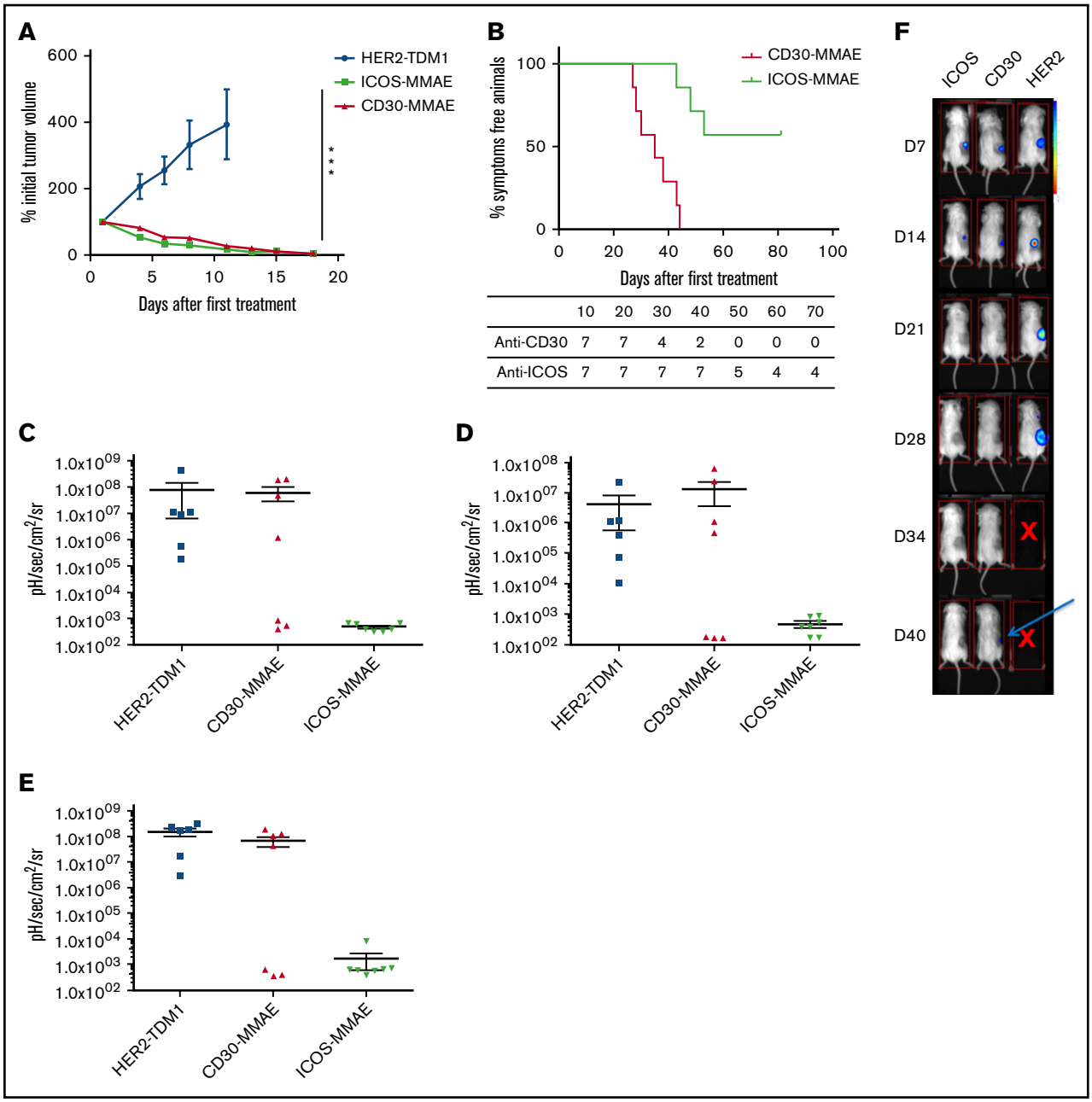

Figure 4. Evaluation of the in vivo efficacy of anti-ICOS-MMAE ADCs in a mouse xenograft model with MyLa cells. (A) Twenty-one mice were engrafted with 8.10^6 MyLa cells each, which were subcutaneously injected with 200 µL phosphate-buffered saline and no basement membrane matrix. Mice were then randomly assigned to 3 groups and monitored for tumor volume after 2 treatments of anti-HER-2, anti-CD30, or anti-ICOS ADCs administered 4 days apart (days 10 and 14 after engraftment). (B) OS curves (Kaplan-Meier) comparing the effect of anti-ICOS and anti-CD30 ADCs. The difference between the 2 curves is significant ($P = .0006$). (C-E) Detection of the development of bioluminescent MyLa metastases in 26 mice assigned to 3 groups and treated with anti-HER2, anti-CD30, or anti-ICOS ADCs in lungs (C), spleen (D), and liver (E). (F) Images of living mice scanned with a luminometer following treatment with anti-HER2, anti-CD30, or anti-ICOS ADCs. At day 40, subcutaneous recurrence was detected in the anti-CD30 ADC group (arrow). ***$P < .001$. D, day.

cytotoxic.[34] In addition, we only identified very few $ICOS^+CD8^+$ T cells in the TME of SS samples, both in the skin and nodes. Although our work was not designed to evaluate the immunomodulatory effect of targeting ICOS with ADCs, we can hypothesize that anti-ICOS mAbs would only inhibit part of the $CD4^+$ and $CD8^+$ lymphocyte pool, and the latter are not effective actors in antitumor immunity in CTCL.

Treg cells are a subpopulation of $CD4^+CD25^+FoxP3^+$ T cells that prevent immune responses to self-antigens, provide immunosuppression, and hence participate in tumor immune escape. Among them, intratumoral $ICOS^+$ Treg cells have a stronger suppressive ability than their $ICOS^-$ counterparts.[35] By secreting interleukin-10 and transforming growth factor β, $ICOS^+$ Treg cells inhibit most innate and adaptive immune cells.[36] Studies of various histological

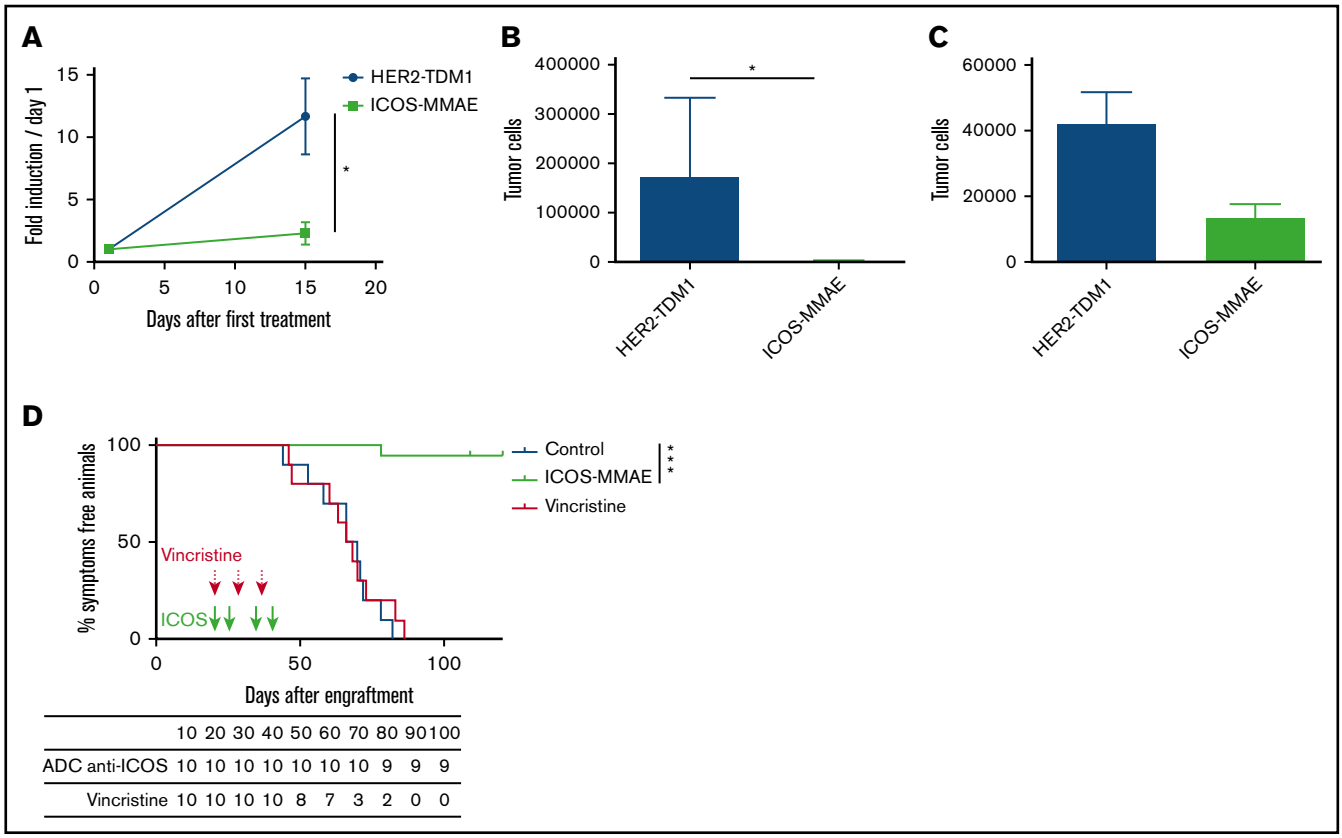

Figure 5. In vivo efficacy of anti-ICOS-MMAE ADCs on ICOS$^+$ PDXs. (A-C) Fourteen mice were engrafted with 5.10^5 cells of PDXs from patients with SS and divided into 2 groups (anti-ICOS-MMAE ADC and anti-HER2 ADC control). Both treatments were injected IV at days 55, 58, 62, and 65 at a dose of 3 mg/kg. Mice were then euthanized at day 69, and organs were removed, dissociated, and analyzed by flow cytometry (in the blood [A], bone marrow [B], and spleen [C]). (D) Thirty mice were engrafted with 5.10^5 cells of PDXs from patients with AITL and divided into 3 groups of 10 mice. Treatment began on day 22, when the earliest blasts were detected in the blood (~0.2 blasts/μL). Anti-ICOS ADC and saline serum (NaCl 0.9%) were injected IV at days 22, 25, 38, and 43 at a dose of 3 mg/kg. Vincristine was administered intraperitoneally on days 22, 29, and 38 at 0.25 mg/kg. *P = .01-.05; ***P < .001.

types of cancer have highlighted the significant numbers of Treg cells in the peripheral blood and TME of patients.[37] Moreover, Le et al[27] demonstrated that follicular B-cell lymphomas generate Treg cells via the ICOS/ICOSL pathway. Here, a significantly higher percentage of Treg cells expressed ICOS in patients with SS than in healthy donors. Targeting ICOS could induce Treg cell depletion, which may improve immune profiles, but further work to address this hypothesis is needed.

ICOS also has an important role in the differentiation and activation of T cells into Tfh cells.[38] Indeed, ICOS mediates the differentiation of Tfh cells through activation of phosphatidylinositol 3-kinase, which promotes persistent motility of T cells.[39] Moreover, costimulation via ICOS induces secretion of interleukin-21 and CXCR5 expression, which are both required for the differentiation and maintenance of Tfh cells and germinal centers and, therefore, the differentiation of B cells.[40] As a matter of fact, the clinical phenotype of ICOS knockout includes common variable immunodeficiency and opportunistic infections.[41] The immunosuppressive potential of ICOS inhibition in patients with CTCL is difficult to predict because, as mentioned above, the T-cell effector immunity of these patients is basically impaired. However, prevention of herpes virus and *Pneumocystis jirovecii* infections in clinical practice would be necessary as in patients on rituximab or long-term systemic corticosteroid therapy.

The rationale for targeting ICOS with ADCs arises from the intrinsic internalizing capacity of ICOS. Indeed, ICOS is rapidly internalized in response to ICOSL engagement, which is necessary for proper T-cell responses.[42] Moreover, unlike antibody-dependent cellular cytotoxicity– and phagocytosis-inducing mAbs, ADCs act directly on tumor cells; the disadvantage is a cumulative toxicity due to the coupled drug, but the advantage is the rapidity of efficiency. Therefore, anti-ICOS ADCs could be used to obtain complete remission before an allograft of hematopoietic stem cells or in cases where a severe clinical manifestation of the disease requires rapid efficacy. Optimizing ADCs to reduce their toxicity and improve their effectiveness is currently under investigation.[43,44]

Our results could be extended to the spectrum of follicular variant PTCL and AITL. These systemic lymphomas, which are the most prevalent, have a poor prognosis, with an OS at 5 years of ~30% and a current chemotherapy regimen that is ineffective in most patients.[45,46] For instance, a phase 1 trial evaluating the tolerance of an antagonistic anti-ICOS antibody with an antibody-dependent cellular cytotoxicity effect, MEDI-570, in patients with relapsed or refractory follicular variant PTCL or AITL was recently initiated

(NCT02520791). To our knowledge, there are no published preclinical data on this mAb or anti-ICOS ADCs.

There is a real unmet need in the treatment of both CTCL and Tfh PTCL. ICOS is a promising therapeutic target, because it is expressed both by tumor T cells and Treg cells. Our results, which expand the strong and frequent expression of ICOS to CTCL, as well as the preclinical efficacy of anti-ICOS ADCs, provide the preliminary basis for a therapeutic trial.

Acknowledgments

The authors thank the patients and their families. The authors thank the Immunity and Cancer team and the TrGet platform at Centre de Recherche en Cancérologie de Marseille for technical assistance.

D.O.'s team was supported by Equipe Fondation Recherche Médicale grant DEQ20180339209. D.O. is a senior scholar of the Institut Universitaire de France. This study was supported by INSERM, Institut Paoli-Calmettes, Fondation ARC pour la Recherche sur le Cancer, and Aix Marseille Université.

Authorship

Contribution: F.A. designed and performed the experiments, analyzed the data, and wrote the manuscript; N.O., S.I.-H.-O., A.D.C., C.S. and P.G. designed and performed the descriptive pathology part of the work, contributed to sample collection from human subjects, and proofread the manuscript; M.L. designed the experiments and proofread the manuscript; F.O. and L.G. performed the experiments; R.C., A.G., and Y.C. designed and performed animal experiments; R.B., J.-M.S., N.B., J.-J.G., and P.B. proofread the manuscript; M.B. and A.B. proofread the manuscript and contributed to sample collection from human subjects; and D.O. supervised the research and provided guidance.

Conflict-of-interest disclosure: D.O. is cofounder and shareholder of ImCheck Therapeutics, Emergence Therapeutics, and Alderaan. M.B. is a member of Takeda's scientific board. M.L. is cofounder and shareholder of Emergence Therapeutics. The remaining authors declare no competing financial interests.

ORCID profiles: N.O., 0000-0003-0111-7422; M.L., 0000-0002-6573-633X; A.D.C., 0000-0002-6902-9288; L.G., 0000-0001-7526-261X; Y.C., 0000-0001-5359-7099; J.-M.S., 0000-0001-9923-4808; A.B., 0000-0002-0409-2497; D.O., 0000-0003-1299-4113.

Correspondence: Florent Amatore, Laboratoire d'Immunologie des Tumeurs, Pr D. Olive, Centre de Recherche en Cancérologie de Marseille, INSERM U1068, 27 Blvd Leï Roure, CS 30059, 13273 Marseille Cedex 09, France; e-mail: florent.amatore@inserm.fr.

References

1. Swerdlow SH, Campo E, Pileri SA, et al. The 2016 revision of the World Health Organization classification of lymphoid neoplasms. *Blood*. 2016;127(20):2375-2390.
2. Jawed SI, Myskowski PL, Horwitz S, Moskowitz A, Querfeld C. Primary cutaneous T-cell lymphoma (mycosis fungoides and Sézary syndrome): part I. Diagnosis: clinical and histopathologic features and new molecular and biologic markers. *J Am Acad Dermatol*. 2014;70(2):205.e1-205.e16, quiz 221-222.
3. Scarisbrick JJ, Hodak E, Bagot M, et al. Blood classification and blood response criteria in mycosis fungoides and Sézary syndrome using flow cytometry: recommendations from the EORTC cutaneous lymphoma task force. *Eur J Cancer*. 2018;93(93):47-56.
4. Roelens M, de Masson A, Ram-Wolff C, et al. Revisiting the initial diagnosis and blood staging of mycosis fungoides and Sézary syndrome with the KIR3DL2 marker. *Br J Dermatol*. 2020;182(6):1415-1422.
5. Bahler DW, Hartung L, Hill S, Bowen GM, Vonderheid EC. CD158k/KIR3DL2 is a useful marker for identifying neoplastic T-cells in Sézary syndrome by flow cytometry. *Cytometry B Clin Cytom*. 2008;74(3):156-162.
6. Ortonne N, Le Gouvello S, Mansour H, et al. CD158K/KIR3DL2 transcript detection in lesional skin of patients with erythroderma is a tool for the diagnosis of Sézary syndrome. *J Invest Dermatol*. 2008;128(2):465-472.
7. Samimi S, Benoit B, Evans K, et al. Increased programmed death-1 expression on CD4+ T cells in cutaneous T-cell lymphoma: implications for immune suppression. *Arch Dermatol*. 2010;146(12):1382-1388.
8. Wada DA, Wilcox RA, Harrington SM, Kwon ED, Ansell SM, Comfere NI. Programmed death 1 is expressed in cutaneous infiltrates of mycosis fungoides and Sézary syndrome. *Am J Hematol*. 2011;86(3):325-327.
9. Klemke CD, Booken N, Weiss C, et al. Histopathological and immunophenotypical criteria for the diagnosis of Sézary syndrome in differentiation from other erythrodermic skin diseases: a European Organisation for Research and Treatment of Cancer (EORTC) Cutaneous Lymphoma Task Force Study of 97 cases. *Br J Dermatol*. 2015;173(1):93-105.
10. Moins-Teisserenc H, Daubord M, Clave E, et al. CD158k is a reliable marker for diagnosis of Sézary syndrome and reveals an unprecedented heterogeneity of circulating malignant cells. *J Invest Dermatol*. 2015;135(1):247-257.
11. Prince HM, Kim YH, Horwitz SM, et al; ALCANZA study group. Brentuximab vedotin or physician's choice in CD30-positive cutaneous T-cell lymphoma (ALCANZA): an international, open-label, randomised, phase 3, multicentre trial. *Lancet*. 2017;390(10094):555-566.
12. Kim YH, Bagot M, Pinter-Brown L, et al; MAVORIC Investigators. Mogamulizumab versus vorinostat in previously treated cutaneous T-cell lymphoma (MAVORIC): an international, open-label, randomised, controlled phase 3 trial. *Lancet Oncol*. 2018;19(9):1192-1204.
13. Bagot M, Porcu P, Marie-Cardine A, et al. IPH4102, a first-in-class anti-KIR3DL2 monoclonal antibody, in patients with relapsed or refractory cutaneous T-cell lymphoma: an international, first-in-human, open-label, phase 1 trial. *Lancet Oncol*. 2019;20(8):1160-1170.
14. Upadhyay R, Hammerich L, Peng P, Brown B, Merad M, Brody JD. Lymphoma: immune evasion strategies. *Cancers (Basel)*. 2015;7(2):736-762.

15. Schietinger A, Greenberg PD. Tolerance and exhaustion: defining mechanisms of T cell dysfunction. *Trends Immunol*. 2014;35(2):51-60.

16. Querfeld C, Leung S, Myskowski PL, et al. Primary T cells from cutaneous T-cell lymphoma skin explants display an exhausted immune checkpoint profile. *Cancer Immunol Res*. 2018;6(8):900-909.

17. Bosisio FM, Cerroni L. Expression of T-follicular helper markers in sequential biopsies of progressive mycosis fungoides and other primary cutaneous T-cell lymphomas. *Am J Dermatopathol*. 2015;37(2):115-121.

18. Amatore F, Gorvel L, Olive D. Inducible co-stimulator (ICOS) as a potential therapeutic target for anti-cancer therapy. *Expert Opin Ther Targets*. 2018; 22(4):343-351.

19. Amatore F, Gorvel L, Olive D. Role of inducible co-stimulator (ICOS) in cancer immunotherapy [published online ahead of print 28 November 2019]. *Expert Opin Biol Ther*. doi:10.1080/14712598.2020.1693540.

20. Marafioti T, Paterson JC, Ballabio E, et al. The inducible T-cell co-stimulator molecule is expressed on subsets of T cells and is a new marker of lymphomas of T follicular helper cell-derivation. *Haematologica*. 2010;95(3):432-439.

21. Buonfiglio D, Bragardo M, Bonissoni S, et al. Characterization of a novel human surface molecule selectively expressed by mature thymocytes, activated T cells and subsets of T cell lymphomas. *Eur J Immunol*. 1999;29(9):2863-2874.

22. Downs-Canner S, Berkey S, Delgoffe GM, et al. Suppressive IL-17A^{+}Foxp3^{+} and ex-Th17 IL-17A^{neg}Foxp3^{+} T_{reg} cells are a source of tumour-associated T_{reg} cells. *Nat Commun*. 2017;8(1):14649.

23. Geskin LJ, Akilov OE, Kwon S, et al. Therapeutic reduction of cell-mediated immunosuppression in mycosis fungoides and Sézary syndrome. *Cancer Immunol Immunother*. 2018;67(3):423-434.

24. Ni X, Jorgensen JL, Goswami M, et al. Reduction of regulatory T cells by Mogamulizumab, a defucosylated anti-CC chemokine receptor 4 antibody, in patients with aggressive/refractory mycosis fungoides and Sézary syndrome. *Clin Cancer Res*. 2015;21(2):274-285.

25. Willemze R, Cerroni L, Kempf W, et al. The 2018 update of the WHO-EORTC classification for primary cutaneous lymphomas. *Blood*. 2019;133(16): 1703-1714.

26. Olsen EA, Whittaker S, Kim YH, et al; Cutaneous Lymphoma Task Force of the European Organisation for Research and Treatment of Cancer. Clinical end points and response criteria in mycosis fungoides and Sézary syndrome: a consensus statement of the International Society for Cutaneous Lymphomas, the United States Cutaneous Lymphoma Consortium, and the Cutaneous Lymphoma Task Force of the European Organisation for Research and Treatment of Cancer. *J Clin Oncol*. 2011;29(18):2598-2607.

27. Le K-S, Thibult M-L, Just-Landi S, et al. Follicular B lymphomas generate regulatory T cells via the ICOS/ICOSL pathway and are susceptible to treatment by anti-ICOS/ICOSL therapy. *Cancer Res*. 2016;76(16):4648-4660.

28. Townsend EC, Murakami MA, Christodoulou A, et al. The public repository of xenografts enables discovery and randomized phase II-like trials in mice [published correction appears in *Cancer Cell* 30(1):183]. *Cancer Cell*. 2016;29(4):574-586.

29. Rubio Gonzalez B, Zain J, Rosen ST, Querfeld C. Tumor microenvironment in mycosis fungoides and Sézary syndrome. *Curr Opin Oncol*. 2016;28(1): 88-96.

30. Nelson MH, Kundimi S, Bowers JS, et al. The inducible costimulator augments Tc17 cell responses to self and tumor tissue. *J Immunol*. 2015;194(4): 1737-1747. doi:10.4049/jimmunol.1401082

31. Faget J, Bendriss-Vermare N, Gobert M, et al. ICOS-ligand expression on plasmacytoid dendritic cells supports breast cancer progression by promoting the accumulation of immunosuppressive CD4+ T cells. *Cancer Res*. 2012;72(23):6130-6141.

32. Nagase H, Takeoka T, Urakawa S, et al. ICOS^{+} Foxp3^{+} TILs in gastric cancer are prognostic markers and effector regulatory T cells associated with *Helicobacter pylori*. *Int J Cancer*. 2017;140(3):686-695.

33. Giraldo NA, Becht E, Vano Y, et al. Tumor-infiltrating and peripheral blood T-cell immunophenotypes predict early relapse in localized clear cell renal cell carcinoma. *Clin Cancer Res*. 2017;23(15):4416-4428.

34. Iliadis A, Koletsa T, Patsatsi A, Georgiou E, Sotiriadis D, Kostopoulos I. The cellular microenvironment and neoplastic population in mycosis fungoides skin lesions: a clinicopathological correlation. *Eur J Dermatol*. 2016;26(6):566-571.

35. Wallin JJ, Liang L, Bakardjiev A, Sha WC. Enhancement of CD8+ T cell responses by ICOS/B7h costimulation. *J Immunol*. 2001;167(1):132-139.

36. Klingenberg R, Autschbach F, Gleissner C, et al. Endothelial inducible costimulator ligand expression is increased during human cardiac allograft rejection and regulates endothelial cell-dependent allo-activation of CD8+ T cells in vitro. *Eur J Immunol*. 2005;35(6):1712-1721.

37. Schenk AD, Gorbacheva V, Rabant M, Fairchild RL, Valujskikh A. Effector functions of donor-reactive CD8 memory T cells are dependent on ICOS induced during division in cardiac grafts. *Am J Transplant*. 2009;9(1):64-73.

38. Stone EL, Pepper M, Katayama CD, et al. ICOS coreceptor signaling inactivates the transcription factor FOXO1 to promote Tfh cell differentiation. *Immunity*. 2015;42(2):239-251.

39. Rolf J, Bell SE, Kovesdi D, et al. Phosphoinositide 3-kinase activity in T cells regulates the magnitude of the germinal center reaction. *J Immunol*. 2010; 185(7):4042. doi:10.4049/jimmunol.1001730

40. Wilcox RA. A three-signal model of T-cell lymphoma pathogenesis. *Am J Hematol*. 2016;91(1):113-122.

41. Schepp J, Chou J, Skrabl-Baumgartner A, et al. 14 years after discovery: clinical follow-up on 15 patients with inducible co-stimulator deficiency. *Front Immunol*. 2017;8:964.

42. Lownik JC, Luker AJ, Damle SR, et al. ADAM10-mediated ICOS ligand shedding on B cells is necessary for proper T cell ICOS regulation and T follicular helper responses. *J Immunol*. 2017;199(7):2305-2315.

43. Dan N, Setua S, Kashyap VK, et al. Antibody-drug conjugates for cancer therapy: chemistry to clinical implications. *Pharmaceuticals (Basel)*. 2018;11(2):E32.

44. Khera E, Thurber GM. Pharmacokinetic and immunological considerations for expanding the therapeutic window of next-generation antibody-drug conjugates [published online ahead of print 21 August 2018]. *BioDrugs Clin Immunother Biopharm Gene Ther*. doi:10.1007/s40259-018-0302-5.

45. Lemonnier F, Couronné L, Parrens M, et al. Recurrent TET2 mutations in peripheral T-cell lymphomas correlate with TFH-like features and adverse clinical parameters. *Blood*. 2012;120(7):1466-1469.

46. Mourad N, Mounier N, Brière J, et al; Groupe d'Etude des Lymphomes de l'Adulte. Clinical, biologic, and pathologic features in 157 patients with angioimmunoblastic T-cell lymphoma treated within the Groupe d'Etude des Lymphomes de l'Adulte (GELA) trials. *Blood*. 2008;111(9):4463-4470.